Cellular/Molecular

Intraflagellar Transport/Hedgehog-Related Signaling Components Couple Sensory Cilium Morphology and Serotonin Biosynthesis in *Caenorhabditis elegans*

Mustapha Moussaif and Ji Ying Sze
Department of Molecular Pharmacology, Albert Einstein College of Medicine, Bronx, New York 10461

Intraflagellar transport in cilia has been proposed as a crucial mediator of Hedgehog signal transduction during embryonic pattern formation in both vertebrates and invertebrates. Here, we show that the Hh receptor Patched-related factor DAF-6 and intraflagellar transport modulate serotonin production in *Caenorhabditis elegans* animals, by remodeling the architecture of dendritic cilia of a pair of ADF serotonergic chemosensory neurons. Wild-type animals under aversive environment drastically reduce DAF-6 expression in glia-like cells surrounding the cilia of chemosensory neurons, resulting in cilium structural remodeling and upregulation of the serotonin-biosynthesis enzyme tryptophan hydroxylase *tph-1* in the ADF neurons. These cellular and molecular modifications are reversed when the environment improves. Mutants of *daf-6* or intraflagellar transport constitutively upregulate *tph-1* expression. Epistasis analyses indicate that DAF-6/intraflagellar transport and the OCR-2/OSM-9 TRPV channel act in concert, regulating two layers of activation of *tph-1* in the ADF neurons. The TRPV signaling turns on *tph-1* expression under favorable and aversive conditions, whereas inactivation of DAF-6 by stress results in further upregulation of *tph-1* independently of OCR-2/OSM-9 activity. Behavioral analyses suggest that serotonin facilitates larval animals resuming development when the environment improves. Our study revealed the cilium structure of serotonergic neurons as a trigger of regulated serotonin production, and demonstrated that a Hedgehog-related signaling component is dynamically regulated by environment and underscores neuroplasticity of serotonergic neurons in *C. elegans* under stress and stress recovery.

Introduction

Stress is a normal part of life experience of every organism, ranging from bacteria to humans. Stress responses are thought to be an ancient genetic program of cellular and physiological plasticity enabling organisms to adjust biological processes according to the environment (Ottaviani and Franceschi, 1996; Leonardo and Hen, 2006). However, molecular mechanisms underlying stress responses remain to be elucidated.

The neurotransmitter serotonin (5-HT) is pivotal in stress responses, because drugs that enhance serotonin signaling are effective in alleviating anxiety. Although 5-HT is continuously biosynthesized in 5-HT neurons, 5-HT levels in the brain and morphology of 5-HT neurons are plastic, and respond to internal and external environmental signals (Azmitia, 1999; Leonardo and Hen, 2006). In rat brain, 5-HT levels in particular regions can be upregulated by particular sensory and physiological stressors (Lee et al., 1987; Chaouloff, 2000).

Hedgehog (Hh) is a family of secreted proteins and has been shown to regulate morphogenesis during embryonic development in both vertebrates and invertebrates (Ingham and McMahon, 2001). In mouse, Sonic Hh signaling regulates the development of 5-HT neurons (Rubenstein, 1998; Briscoe et al., 1999; Pattyn et al., 2003). Recent studies established that intraflagellar transport (IFT), a microtubule-based machinery moving protein cargos in and out of nonmotile cilia of cells (Rosenbaum and Witman, 2002; Scholey, 2003), is a crucial mediator of Hh signaling transduction (Huangfu et al., 2003; Corbit et al., 2005; Tran et al., 2008). Mutations in IFT perturb mouse embryonic patterning by blocking Hh receptor Patched-1 signaling (Huangfu et al., 2003).

Here, we show that Patched DAF-6, Dispatched DAF-14, and IFT modulate 5-HT production in *Caenorhabditis elegans* animals, by modifying cilium architecture of serotonergic neurons. ADFs are the only 5-HT sensory neurons in *C. elegans* hermaphrodites. ADFs reside in a pair of amphid sensilla in the head region. Each amphid comprises one ADF, 11 other sensory neurons, and two supporting cells, a socket and a glia-like sheath, which form a channel surrounding the cilia at the dendritic tips of the sensory neurons; the cilia of ADF and seven other sensory neurons pass through the amphid channel to access the external environment (Ward et al., 1975). DAF-6 and DAF-14 are expressed in the channel, whereas IFT components are expressed in the cilia (Michaux et al., 2000; Perens and Shaham, 2005; Inglis et al., 2007). Importantly, amphid architecture is dynamically modulated by environment. Under harsh conditions, worms develop-

Received Jan. 5, 2009; revised Feb. 19, 2009; accepted Feb. 19, 2009.

This work was supported by a grant from the National Institutes of Mental Health (to J.Y.S.). We thank R. Horvitz, C. Bargmann, T. Stiernagle, and the *Caenorhabditis* Genetics Center for worm strains and the *C. elegans* Knockout Consortium for deletion mutants. We are grateful to S. Shaham for unpublished DAF-6::GFP transgenic lines, which made the study possible.

Correspondence should be addressed to Ji Ying Sze, Department of Molecular Pharmacology, Albert Einstein College of Medicine, 202 Golding Building, 1300 Morris Park Avenue, Bronx, NY 10461. E-mail: jsze@aecom.yu.edu.

DOI:10.1523/JNEUROSCI.0044-09.2009

 0270-6474/09/294065-11$15.00/0

mentally arrest as morphologically distinct dauer larvae. Dauers remodel the architecture of amphid cilia and channel (Albert and Riddle, 1983), alter the expression of specific chemosensory receptors (Peckol et al., 2001), and turn on many homeostatic stress response genes (Hu, 2007). When the environment improves, dauers recover, revert cilium structural modifications, and resume development. We show that dauers remodel the amphid architecture by downregulating DAF-6 expression, and amphid structural modifications trigger upregulation of the tryptophan hydroxylase gene *tph-1* in ADF. Mutants of DAF-6 or IFT constitutively upregulate *tph-1*. Our studies establish that Hh-like signaling components are dynamically regulated in an animal by the environment, and underscore cilium structural plasticity, which in turn governs 5-HT production in chemosensory neurons.

Materials and Methods

Worm strains. C. elegans strains were maintained under standard culture conditions on NGM agar plates with *Escherichia coli OP50* as a food source (Brenner, 1974). Strains were obtained from the Caenorhabditis Genetic Center (CGC) unless noted. Wild-type (WT) animals were the Bristol Strain *N2*. The Hawaiian isolate *CB4856* was used for genetic mapping the *dyf-1(yz66)* and *dyf-12(yz67)* mutations. Mutants used were as follows: *che-2(e1033)*, *che-3(e1124)*, *che-11(e1810)*, *che-13(e1805)*, *che-14(ok193)*, *daf-3(mgDf90)*, *daf-6(p675)*, *daf-12(m583)*, *daf-16(mgDf50)*, *dyf-1(mn335)*, *dyf-12(sa127)*, *egl-30(js126gf)*, *egl-30(tg26gf)*, *egl-30(ad806lf)*, *goa-1(n363)*, *gpa-10(pk362)*, *gpa-13(pk1270)*, *itr-1(sa73)*, *kap-1(ok676)*, *mec-12(e1605)*, *ocr-2(yz5)* and *osm-9(yz6)* (isolated in our laboratory), *ocr-2(ak47)* and *ocr-2(ak47) osm-9(ky10)* (kindly provided by C. Bargmann, Rockefeller University, New York, NY), *osm-3(p802)*, *osm-12(n1606)* (also known as *bbs-7*), *tax-2(p671)*, *tax-6(p675lf)*, *tax-6(jh107gf)*, *tba-9(ok1858)*, and MT15434 *tph-1(mg280)* (kindly provided by R. Horvitz, Massachusetts Institute of Technology, Cambridge, MA); and *unc-2(e55)* and *unc-43(e408)*.

Isolation and mapping of dyf-1(yz66) *and* dyf-12(yz67). The *yz66* and *yz67* mutations were isolated from a genetic screen for mutants that can turn on GFP expression in the ADF chemosensory neurons after ethyl methane sulfonate mutagenesis of *ocr-2(yz5)* mutant carrying an integrated *tph-1::gfp* transgene. *yz66*, *yz67*, and 43 other independent mutants were isolated from screening estimated 12,200 mutagenized haploid genomes. Recovery of 5-HT in the mutants was validated by anti-5-HT antibody staining. 1,1′-Dilinoleyl-3,3,3′,3′-tetramethylindocarbocyanine perchlorate (DiI) staining was initially used to examine the amphid morphology in the mutants. *yz66*, *yz67*, and 36 of the other mutants were found to be dye-filling defective (Dyf). The Dyf phenotype was particularly intriguing because *tph-1::gfp* expression and anti-5-HT antibody staining suggested that the mutations did not alter ADF cell fates and because published work showed Dyf mutants exhibiting stress phenotypes (Apfeld and Kenyon, 1999; Lin et al., 2001). Using the SNP map of *CB4856*, we localized *yz66* between the polymorphisms F57C9 and F57G9 on the chromosome I, and *yz67* between T22A3 and F11A1 on X. Noncomplementation assays with Dyf mutants within these regions revealed that *yz66* and *yz67* mutations are allelic to *dyf-1* and *dyf-12*, respectively. The molecular lesion of *yz66* was determined by sequencing *dyf-1* coding sequences amplified from the mutant genome, which revealed a 168 bp deletion predicting to remove 56 aa from position 362 to 417 plus V418L substitution in the context of the *dyf-1(l)* isoform (see Fig. 2*b*).

Construction of dyf-1 *transgenes.* All the constructs were generated by PCR. *dyf-1(g)* is a genomic fragment amplified from the WT genome encompassing 465 bp 5′-upstream promoter sequence, exons/introns, and 581 bp 3′-untranslated region (UTR), as described previously (Ou et al., 2005).

To express *dyf-1* in specific neurons, we fused *dyf-1* cDNA sequences to heterologous promoters. We prepared cDNA mixture from total RNA of WT animals, using a reverse transcription kit (Invitrogen). *dyf-1(l)* and *dyf-1(s)* were amplified from the cDNA mixture using isoform-specific primers. *ADF::dyf-1* is a fusion gene that contains 3.5 kb 5′-upstream promoter of the *srh-142* gene, a *dyf-1* cDNA sequence, and *unc-54* 3′-UTR from the plasmid pPD95.75 (from A. Fire, Stanford University School of Medicine, Stanford, CA). This *srh-142* promoter directs an ADF-specific expression (Sagasti et al., 1999; S. Zhang et al., 2004). *Pgpa-11::dyf-1* is a fusion of 3.5 kb promoter of the *gpa-11* gene, *dyf-1 cDNA*, and *unc-54* 3′-UTR. *gpa-11* is expressed specifically in the ASH and ADL neurons (Jansen et al., 1997). Individual constructs were coinjected with an *elt-2::gfp* transgenic marker (kindly provided by J. McGhee, University of Calgary, Calgary, Alberta, Canada) into *dyf-1(yz66);ocr-2(yz5)* animals expressing an integrated *tph-1::gfp* reporter. Rescue of *dyf-1(yz66)* phenotype was assayed by the ability of the transgenes to restore the *ocr-2(yz5)* 5-HT phenotype in the ADF neurons on one hand and to rescue the dye-filling defective phenotype on the other hand.

Quantification of tph-1::gfp *expression and anti-5-HT antibody staining.* The expression of an integrated *tph-1::gfp* reporter in the ADF neurons in living WT or mutant animals was assessed by quantifying GFP intensity. Images of individual neurons were captured with an AxioCam digital camera and the AxioVision software (Zeiss) at a fixed exposure time, and the intensity of the fluorescence within a fixed pixel area of the cell body was quantified using Adobe Photoshop. All the animals examined were L3–L4 larvae, unless noted otherwise. Mutants were always compared with WT animals grown under the same conditions. For example, *daf-2* non-dauer animals and WT animals grown at 15°C were compared, and *daf-2* dauers, WT dauers (induced by the pheromone), and WT non-dauers (absence of the pheromone) grown at 25°C were compared. The data are based on comparisons between WT and mutant strains assayed in parallel. Because L4 larvae are bigger than dauers, the cell body in an L4 larva might be slightly bigger than that of its counterpart cell in a dauer. To ensure that the increase of the GFP intensity in dauers was not due to the smaller cell body, we quantified GFP intensity in the entire ADF neuron, using the NIH ImageJ Software version 1.38x. The ratios of the GFP intensity in the entire ADF of L4 versus that in dauers (data not shown) were comparable to the data from quantifications of a fixed pixel area within the cell bodies. Two independent integrated *tph-1::gfp* transgenes in dauers were examined, and the results were comparable. The data derived from one *tph-1::gfp* transgene are presented.

Whole-mount staining with anti-5-HT antibody was performed as previously described (Sze et al., 2000). For all the strains, the *tph-1::gfp* transgene was outcrossed before the staining.

Dauer assay conditions. Dauers were prepared as previously described (Golden and Riddle, 1984). Briefly, 2 ml of NGM agar prepared without peptone, containing 3 U of crudely purified dauer pheromone and 50 μg/ml streptomycin, was placed in a 35 mm Petri plate. After agar solidification, 20 μl of 5% (wt/v) suspension of *E. coli OP50* preheated at 95°C for 25 min in S-medium containing 50 μg/ml streptomycin was placed on the agar surface. Fifteen to twenty gravid worms were allowed to lay eggs for 3 h then removed from the plates, laid eggs were incubated for 72 h at 25°C, and resultant dauers were examined. To test dauer recovery, 30 dauers from a strain were transferred to a fresh plate without the pheromone and incubated at 25°C; animals that resumed pharyngeal pumping were scored as recovered.

Heat shock treatment. Five gravid worms from a strain were transferred to a NGM plate seeded with *OP50* food and incubated at 20°C for 72 h to produce progeny. The plates were then shifted to 37.5°C for 90 min and returned to 20°C for 6–8 h. *tph-1::gfp* expression in the ADF neurons of survived L3–L4 larvae was quantified.

8-Bromo-cGMP assays. The assay medium plates and the concentrations of 8-bromo-cGMP were prepared according to a published procedure (Birnby et al., 2000). Fifteen to twenty gravid worms were allowed to lay eggs for 3 h and then removed from the plates. The plates were incubated at 20°C for 48 h before the animals were scored for *tph-1::gfp* expression in the ADF neurons.

Dye-filling assays. Well-fed animals were incubated at room temperature for 30–120 min in the lipophilic dye DiI adjusted to a final concentration of 10 μg of DiI per milliliter of M9 buffer. Animals were washed three times with M9 buffer before being analyzed under fluorescence microscopy.

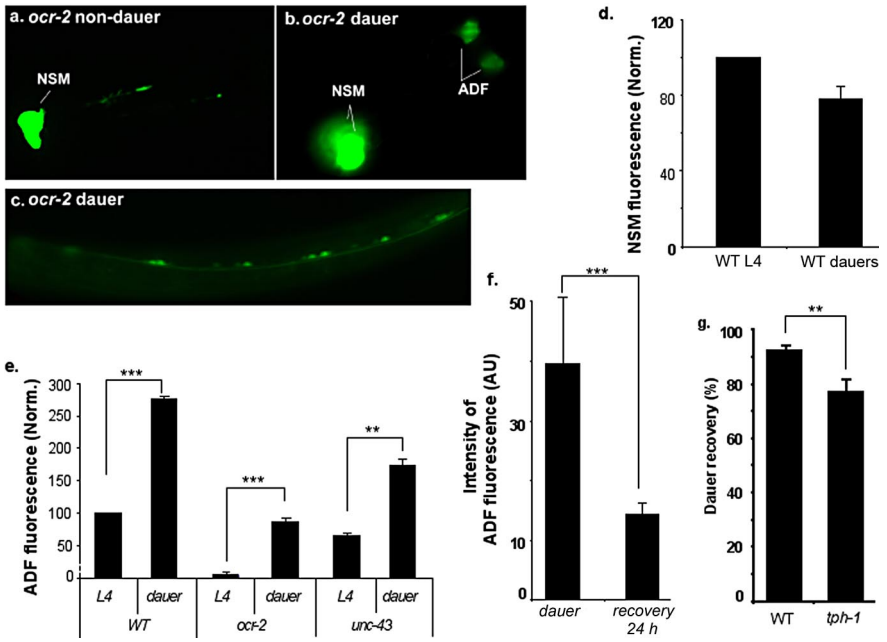

Figure 1. *tph-1::gfp* expression is upregulated in dauers. ***a–c***, Representative photomicrographs showing *tph-1::gfp* expression in *ocr-2* mutant background. ***a***, GFP fluorescence was not visible in ADF in an L4 larva. ***b***, GFP fluorescence in the ADF neurons was restored in a dauer. ***c***, GFP fluorescence was induced in the ventral cord motor neurons in a dauer. ***d***, ***e***, Quantification of *tph-1::gfp* expression in dauer and non-dauer animals. Average fluorescence in NSM (***d***) and ADF (***e***) neurons, normalized to that in WT L4 larvae, is shown for WT dauers and mutants. Each bar represents at least three independent experiments ± SEM, with 10–15 animals per strain per condition per experiment. Values of dauers that differ significantly from that of non-dauers of the same strain are indicated (**$p < 0.01$; ***$p < 0.001$, Student's *t* test). The fluorescence intensity in the NSM neurons was not significantly lower in dauers ($p > 0.05$, Student's *t* test). ***f***, Quantification of *tph-1::gfp* expression in dauers and after dauer recovery. *ocr-2(yz5)* was used in this experiment to separate activation of *tph-1* expression by the OCR-2/OSM-9 channel from dauer-induced upregulation. *ocr-2* mutants were induced to form dauers by applying the dauer pheromone. A portion of the dauers was transferred to normal NGM plates for recovery for 24 h, and *tph-1::gfp* expression in animals that resumed pharyngeal pumping was analyzed and compared with that in dauers remaining on the pheromone-containing plates. The assay has been performed multiple times, and the data from one experiment are presented. Number of animals analyzed: 31 dauers and 54 recovered from dauers. AU, Arbitrary units. ***g***, *tph-1* mutants exhibit a delay in dauer recovery. WT and *tph-1* mutant larvae were induced to form dauers by applying the dauer pheromone. The resultant dauers were allowed to recover on fresh culture plates without the pheromone for 7–8 h. The animals that resumed rhythmic pharyngeal pumping were scored as recovered. Each bar represents the summary of five independent experiments ± SEM, with 30–40 animals per strain per experiment (**$p < 0.01$, Student's *t* test).

Results

tph-1 expression is upregulated in the ADF chemosensory neurons of dauers

The tryptophan hydroxylase gene *tph-1* is required for 5-HT biosynthesis in *C. elegans* (Sze et al., 2000). We have been using a stably integrated *tph-1::gfp* reporter to monitor *tph-1* expression in living *C. elegans* worms. In WT larvae, *tph-1::gfp* is predominantly expressed in two classes of neurons: a pair of ADF chemosensory neurons and a pair of NSM pharyngeal secretory neurons, and *tph-1::gfp* is expressed additionally in a pair of egg-laying motor neurons HSN in adult hermaphrodites (Sze et al., 2000). Studies from our laboratory and others have demonstrated that the intensity of *tph-1::gfp* expression reflects the cellular 5-HT levels detected by anti-5-HT antibody staining (S. Zhang et al., 2004; Y. Zhang et al., 2005).

Previously, we have reported that the OCR-2 and OSM-9 TRPV channel proteins act cell autonomously to regulate *tph-1* expression in the ADF neurons (S. Zhang et al., 2004). The *ocr-2(yz5)* allele was isolated based on reduced *tph-1* expression in ADF in animals grown under optimal growth conditions. During the course of phenotypic characterization of this neuron-specific 5-HT synthesis mutant, we made a surprise observation that *tph-1::gfp* expression was restored when *ocr-2(yz5)* mutants were induced to form dauers by aversive growth conditions (Fig. 1*b*,*e*). To ensure that the restoration of *tph-1::gfp* expression was not an allelic-specific artifact, we examined *ocr-2(ak47)* deletion, *osm-9(yz6)* null, and *ocr-2(ak47); osm-9(ky10)* double mutant animals. *tph-1::gfp* expression in the ADF neurons was restored in all these mutants when they became dauers (data not shown). CaMKII UNC-43 has been implicated as a downstream component of OCR-2/OSM-9 TRPV signaling, and *unc-43* loss-of-function (lf) mutations reduce *tph-1::gfp* expression in the ADF neurons under optimal growth conditions (S. Zhang et al., 2004). *tph-1::gfp* expression also was restored in *unc-43(lf)* dauers (Fig. 1*e*).

The restoration of *tph-1::gfp* expression in *ocr-2* and *osm-9* dauers could reflect another layer of *tph-1* activation that is repressed under optimal growth conditions. Alternatively, dauers might alter neuronal programs so that the TRPV channel signaling is no longer needed. If dauers derepress an independent mechanism, we should expect *tph-1::gfp* expression in ADF neurons to be upregulated in WT dauers. If dauers simply bypass the TRPV channel, *tph-1::gfp* expression levels would be equivalent between WT dauers and non-dauers. To distinguish between these two possibilities, we examined *tph-1::gfp* expression in WT dauers. We induced WT larvae to form dauers by starvation or applying the dauer-inducing pheromone. The control was WT worms growing in parallel but with food and without the pheromone. *tph-1::gfp* expression in the ADF neurons of the dauers was on average 2.8-fold higher than that in their non-dauer siblings (Fig. 1*e*). In addition, *tph-1::gfp* was ectopically induced in the ventral motor neurons in WT dauers as well as in *ocr-2* and *osm-9* mutant dauers (Fig. 1*c*; data not shown). However, *tph-1::gfp* expression levels in the NSM neurons were not significantly affected (Fig. 1*d*). Furthermore, the increase in *tph-1::gfp* expression in ADF and the expression in the motor neurons both were diminished within 24 h after the dauers were allowed to recover under optimal growth conditions (Fig. 1*f*). We concluded that dauers do not simply suppress the mutations of the TRPV channel; rather, they activate a genetically separable mechanism to upregulate *tph-1* expression in ADF and induce *tph-1* expression in additional neuronal classes.

Serotonin promotes dauer recovery when the environment improves

What could be the physiological role of this upregulation of 5-HT production? Previous studies suggested that 5-HT modulates dauer/non-dauer switch. *tph-1* deletion mutants, containing no detectable 5-HT, promote dauer formation (Sze et al., 2000). Conversely, applying exogenous 5-HT facilitates dauer recovery of weak dauer-constitutive mutants, although it cannot prevent

the mutants from forming dauers (Daniels et al., 2000). We further tested the role of endogenous 5-HT in dauer recovery. We induced WT and *tph-1* mutants to form dauers by applying the dauer pheromone, and resultant dauers were allowed to recover on fresh culture plates without the pheromone. Most WT dauers recovered and resumed pharyngeal pumping within 2–3 h after they were transferred to the fresh medium, consistent with previous studies (Cassada and Russell, 1975). However, ~25% *tph-1* dauers did not pump even after 7–8 h (Fig. 1*g*). These results suggest that 5-HT may have a role in facilitating worms to resume a normal life when stress signals no longer exist.

dyf-1 in the sensory cilia of the ADF neurons regulates *tph-1* expression

To identify the mechanism underlying *tph-1* upregulation in animals under aversive conditions, we performed a mutagenesis screen for mutants that decouple this gene–environment interaction, thereby constitutively upregulating *tph-1* expression. In *ocr-2* mutants under optimal growth conditions, *tph-1::gfp* expression in the ADF neurons is not visible under a dissecting fluorescence microscope, but *tph-1::gfp* in ADF can be clearly observed in *ocr-2* dauers (Fig. 1*a*,*b*). We mutagenized *ocr-2(yz5)* mutants carrying the *tph-1::gfp* reporter and retrieved mutants that can turn on *tph-1::gfp* in ADF even under non-dauer conditions. Genetic mapping and subsequent complementation analyses revealed that two of the mutants, *yz66* and *yz67*, are, respectively, an allele of *dyf-1* and an allele of *dyf-12* mutants. Both *dyf-1* and *dyf-12* were previously known as amphid cilium mutants because of their defects in taking up lipophilic dyes. When living WT worms are soaked in a solution containing the lipophilic dye DiI, dye fills in six pairs of the exposed amphid chemosensory neurons, but *dyf-1*, *dyf-12*, and other cilium mutants fail in dye filling (Dyf) (Fig. 2*c*) (Starich et al., 1995). *dyf-1* encodes a conserved cilium protein and functions in the anterograde IFT to move cargo proteins along the microtubule-based axoneme to the distal ciliary segments (Ou et al., 2005). Sequencing of the mutant genome established that *yz66* is an in-frame deletion predicting to remove 56 aa in a conserved prenyltransferase domain (Fig. 2*b*). The molecular identity of *dyf-12* has not yet been defined.

To ensure that the Dyf mutations indeed restored 5-HT production in *ocr-2* mutant background, we stained mutant worms with anti-5-HT antibody. ADF 5-HT immunoreactivity was dramatically reduced although not eliminated in *ocr-2(yz5)* mutants, as previously reported (S. Zhang et al., 2004). However, almost all *ocr-2(yz5);dyf-1(yz66)* and *ocr-2(yz5);dyf-12(yz67)* double mutants exhibited strong ADF 5-HT immunoreactivity (Fig. 2*c*,*e*). Judged by both *tph-1::gfp* expression and anti-5-HT antibody staining, *dyf-1* and *dyf-12* mutations did not have a discernable effect on any other 5-HT neurons (Fig. 2*c*,*g*,*h*; data not shown). Two sets of other experiments further affirmed the role of *dyf-1* and *dyf-12* in regulating *tph-1* expression. First, other alleles, *dyf-1(mn335)* and *dyf-12(sa127)*, also restored *tph-1::gfp* expression and 5-HT immunoreactivity in *ocr-2(yz5)* background (Fig. 2*e*, Table 1). Second, a *dyf-1(g)* transgene, which contains a 5.9 kb genomic sequence of the WT *dyf-1* gene, both rescued the dye-filling defects and reverted the effects on *tph-1* expression, namely *dyf-1(yz66);ocr-2(yz5)* transgenic animals exhibited low levels of *tph-1::gfp* expression in ADF as seen in *ocr-2(yz5)* alone (Fig. 2*c*,*f*). These results suggest that *dyf-1* activity normally represses *tph-1* expression in the ADF neurons.

Because *dyf-1* and *dyf-12* mutations affect the cilia of ADF as well as other sensory neurons in the amphids, we investigated the cellular sites of DYF-1 action required to repress *tph-1* expression. The *dyf-1* gene encodes two isoforms, *dyf-1(l)* and *dyf-1(s)*, with *dyf-1(l)* containing 59 more amino acids at the N terminus (Fig. 2*b*) (Ou et al., 2005). We expressed individual isoforms specifically in the ADF neurons (*ADF::dyf-1*) or in the ASH and ADL neurons (*Pgpa-11::dyf-1*). Four *ADF::dyf-1(l)* transgenic lines all significantly reverted the effect of *dyf-1* mutations on *tph-1::gfp* expression (Fig. 2*d*,*f*), but seven *ADF::dyf-1(s)* transgenic lines did not (data not shown). By contrary, none of seven *Pgpa-11::dyf-1(l)* transgenic lines had an appreciable effect on *tph-1::gfp* expression, although they could fully restore dye filling in the ASH and ADL neurons (Fig. 2*d*). Thus, *dyf-1* activity in the ADF neurons is required to repress *tph-1* expression. However, the *ADF::dyf-1(l)* transgene did not fully reinstitute the repression as the *dyf-1(g)* transgene did. This could be due to lower expression levels of the cDNA sequence. Alternatively, the defective cilia of other chemosensory neurons in *dyf-1* mutant background may influence the cilium structure and activity of ADF.

tph-1 expression in the ADF neurons is upregulated in many IFT mutants

Dendritic cilia are thought to function as a matrix for sensory signaling molecules that translate chemical and physical stimuli into neuronal signals (Perkins et al., 1986; Rosenbaum and Witman, 2002; Scholey and Anderson, 2006). Because *dyf-1* and *dyf-12* mutations were identified based on the restoration of *tph-1* expression in *ocr-2* mutant background, we asked whether Dyf mutants simply suppress *tph-1* downregulation by the *ocr-2(yz5)* mutation or derepress a distinct regulatory mechanism, as seen in dauers. To address this question, we outcrossed *ocr-2(yz5)* mutation from the mutants, and examined *tph-1* expression by Dyf mutations on their own. Under optimal growth conditions, *tph-1::gfp* expression in the ADF neurons was ~2.5-fold higher in *dyf-1(yz66)* mutants at L3–L4 stages than that in age-matched WT animals (Fig. 3). Noticeably, *tph-1::gfp* expression levels in the ADF neurons of *dyf-1* mutants grown under optimal growth conditions were comparable to that in WT dauers. Thus, *dyf-1* mutants upregulate *tph-1::gfp* expression in the ADF neurons.

We next investigated the relationship between upregulation of *tph-1* expression by Dyf mutations and the downregulation by mutations of the OCR-2/OSM-9 TRPV channel. Because *ocr-2(yz5)* allele is a missense mutation, we generated *dyf-1;ocr-2(ak47)*-deletion and *dyf-1;osm-9(yz6)*-null double and *dyf-1;ocr-2(ak47);osm-9(ky10)* triple mutants. *tph-1::gfp* expression in the ADF neurons in these genetic backgrounds was comparable to that in *dyf-1;ocr-2(yz5)* (Fig. 3). Therefore, like dauers (Fig. 1), *dyf-1* mutants can upregulate *tph-1::gfp* expression independently of the TRPV channel.

IFT is a microtubule-based motility in which motor proteins and other IFT components assemble to particles moving protein cargos in and out of the cilium, thereby delivering cilium precursors, secretory proteins, chemosensory receptors, and signaling components to the sensory endings. Genetics, electron microscopy (EM), and cellular analyses have identified essential IFT components as well as proteins of specific tasks in particular ciliary segments (Perkins et al., 1986; Blacque et al., 2005; Scholey and Anderson, 2006; Inglis et al., 2007). We asked whether *tph-1* expression is regulated via specific IFT components, such as DYF-1, or is governed by the structure of the cilium. To discern these possibilities, we examined dye filling of the amphid neurons and *tph-1::gfp* expression in a series of available mutants (Blacque et al., 2005) of identified IFT components: *osm-3* (kinesin, anterograde motor), *che-2* (IFT particle B), *che-11* (particle A), *che-13* (particle B), *bbs-7* (distal segment assembly), *che-3* (dynein heavy chain, retrograde motor), *kap-1* (heteromeric

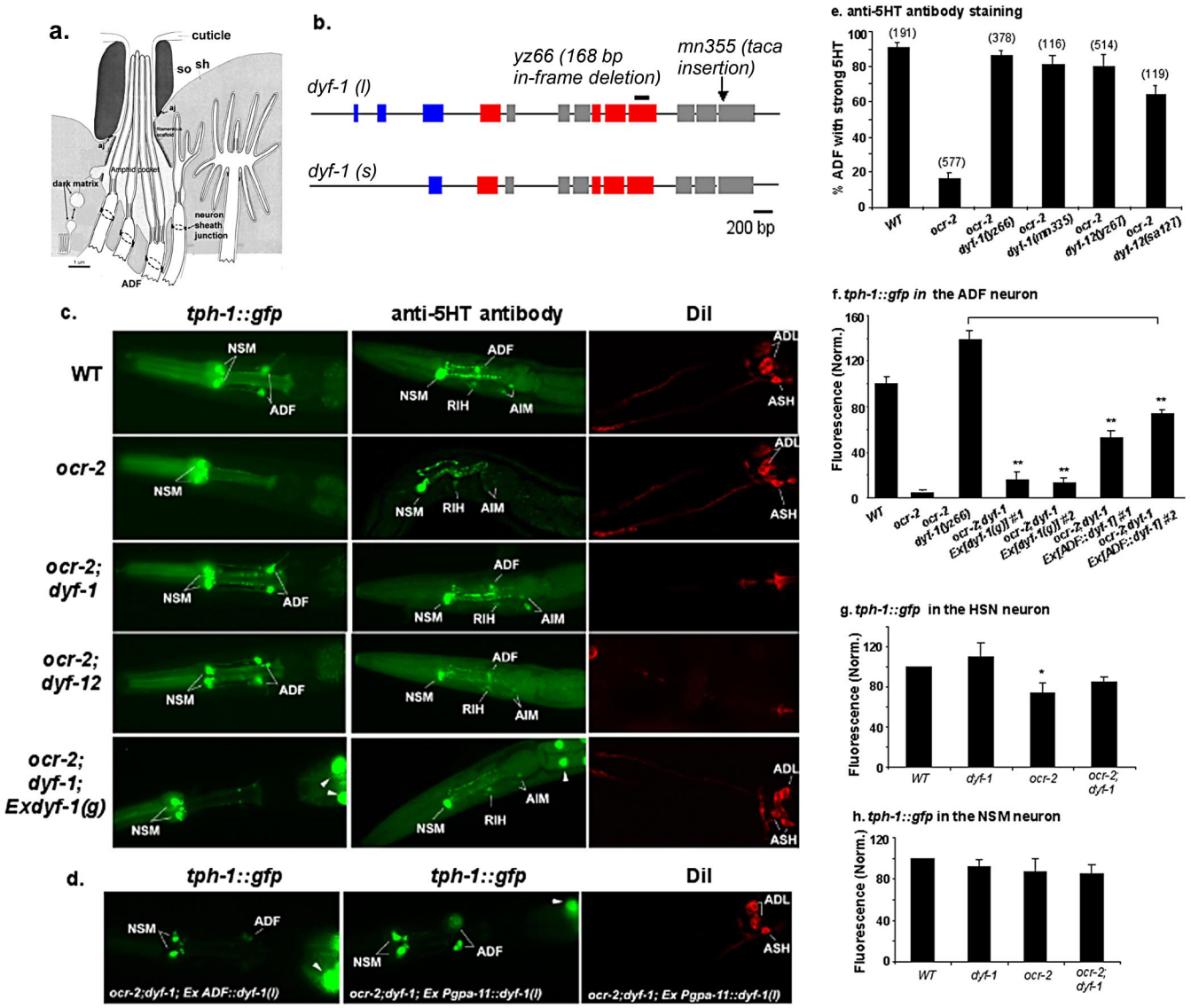

Figure 2. *tph-1::gfp* expression in IFT mutants *dyf-1* and *dyf-12*. ***a***, A schematic depiction of a longitudinal section of the amphid sensillum in WT. Two support cells, a socket (so) and a sheath (sh), form a channel around the ciliated portion of the dendrites of the chemosensory neurons. In the sheath cell, the Golgi apparatus gives rise to dark matrix-filled vesicles, which are secreted to fill in the posterior space between the cilia and the channel. The ciliary endings of ADF and seven other classes of the chemosensory neurons are exposed to the external environment. The sheath cell is connected by adherent junctions (aj) to the sensory dendrites as well as to the socket cell. The socket cell is also connected to the cuticle at the opening pore. [This panel was modified, with permission, from Perkins et al. (1986).] ***b***, The structure of the *dyf-1* gene. Boxes and lines denote, respectively, exons and introns. *dyf-1(l)* and *dyf-1(s)* are two transcriptional isoforms. The mutation sites are shown. Blue boxes, Tetratricopeptide repeat; red boxes, prenyltransferase domain (Ou et al., 2005). ***c***, Photomicrographs showing *tph-1::gfp* expression, anti-5-HT antibody staining, and DiI staining of *dyf-1* and *dyf-12* mutants. *dyf-1(yz66)* and *dyf-12(yz67)* mutants failed dye filling, but both increased *tph-1::gfp* expression and anti-5-HT immunoreactivity in the ADF neurons in *ocr-2* mutant background. A transgene containing the WT *dyf-1* genomic region (*dyf-1(g)*) rescued all these *dyf-1* mutant phenotypes. ***d***, Photomicrographs of *dyf-1;ocr-2* double mutants expressing the *dyf-1(l)* isoform in specific neurons. The *ADF::dyf-1(l)* transgene was sufficient to revert *tph-1::gfp* upregulation, whereas the *Pgpa-11::dyf-1(l)* transgene did not produce an effect on *tph-1::gfp* expression in the ADF neurons, although it can restore dye filling in the ADL and ASH neurons. All the animals shown are L4 larvae, with the anterior toward the left. ***e***, ADF 5-HT immunoreactivity in *dyf-1* and *dyf-12* mutants. Strong 5-HT is defined as the immunoreactivity similar to that seen in WT shown in ***c***. Each bar represents the summary of three staining trials ± SEM, and the number of animals analyzed for each strain is indicated on the top of the bar. L3–L4 larvae were analyzed. ***f–h***, Quantification of *tph-1::gfp* expression in *dyf-1* mutant background. Average fluorescence in indicated neuronal types, normalized to that in WT, is shown for the mutants. Two independent transgenic lines for *Ex[dyf-1(g)]* and *Ex[ADF::dyf-1(l)]* were analyzed. The data are based on values of the NSM and ADF neurons in L3–L4 larvae, and that of HSN in 1-d-old young adults. Each bar represents the summary of three independent experiments ± SEM, with 10–15 animals per strain per experiment. **Significant difference between transgenic animals and *ocr-2;dyf-1(yz66)* mutants ($p < 0.01$, Student's *t* test). *Significant difference between WT and *ocr-2* mutants ($p < 0.05$, Student's *t* test).

kinesin-II accessory protein), *osm-3* (kinesin-II), *tba-9* (β-tubulin), and *mec-12* (α-tubulin). Although the intensities of *tph-1::gfp* in the ADF neurons vary among IFT mutants, a simple conclusion from the results is that the expression of *tph-1::gfp* in ADF neurons was significantly increased in all IFT mutants that were dye-filling defective, but not in those that preserved dye-filling ability (Table 1), pointing to the cilium structure as an important determinant for the changes in *tph-1* expression.

Classic dauer-inducing transcription factors are not required for *tph-1* upregulation in dauers and IFT mutants

While Dyf mutants do not physically form dauers, they share certain aspects with dauers. Dauer formation is a result of a series of structural and functional modifications in neuronal and non-neuronal systems specialized for survival under harsh conditions. Formation of dauers requires activation of at least one of several transcription factors, including DAF-16/FoxO, DAF-3/SMAD,

Table 1. Quantification of *tph-1::gfp* expression in the ADF neurons

Strains	DiI	Relative GFP intensity in ADF (%)	*N*
Wild type	+	100	143
ocr-2(yz5)	+	5.2 ± 0.3[a]	22
ocr-2(ak47)	+	6.6 ± 0.7[a]	22
IFT mutants			
bbs-7;ocr-2(yz5)	−	90.1 ± 17.5[b]	36
bbs-7	−	311.0 ± 2.9[a]	32
che-2;ocr-2(yz5)	−	148.7 ± 10.8[b]	45
che-2	−	252.0 ± 23.4[a]	42
che-3;ocr-2(yz5)	−	135.4 ± 0.4[b]	56
che-11;ocr-2(yz5)	−	123.7 ± 1.1[b]	52
che-11	−	225.4 ± 6.93[a]	77
che-13;ocr-2(yz5)	−	132.4 ± 29.1[b]	41
che-13	−	201.0 ± 9.0[a]	42
dyf-1(yz66);ocr-2(yz5)	−	141.3 ± 7.0[b]	40
dyf-1(yz66)	−	255.1 ± 15.4[a]	39
dyf-1(mn335);ocr-2(yz5)	−	163.5 ± 16.8[b]	36
osm-3;ocr-2(yz5)	−	67.5 ± 2.9[b]	37
osm-3	−	189.1 ± 7.5[a]	56
kap-1;ocr-2(yz5)	+	6.3 ± 1.4[c]	23
kap-1	+	99.9 ± 5.8[d]	112
mec-12;ocr-2(yz5)	+	5.5 ± 0.6[c]	24
mec-12	+	100.7 ± 3.5[d]	103
tba-9;ocr-2(yz5)	+	5.8 ± 1.2[c]	30
tba-9	+	88.7 ± 8.3[d]	63
Hh signaling components			
daf-6;ocr-2(yz5)	−	70.2 ± 4.6[b]	58
daf-6	−	186.3 ± 23.7[a]	60
che-14;ocr-2(yz5)	+/−	37.7 ± 1.3[b]	67
che-14	+/−	133.5 ± 6.0[a]	61
Sensory mutants			
tax-2;ocr-2(yz5)	na	5.9 ± 0.6[c]	23
tax-2	na	72.6 ± 7.1[d]	99
tax-2;che-2;ocr-2(yz5)	na	119.5 ± 6.4[b]	53
tax-6(lf);ocr-2(ak47)	na	6.3 ± 0.6[c]	23
tax-6(lf)	na	100.2 ± 11.0[d]	43
tax-6(lf);daf-6;ocr-2(ak47)	na	83.4 ± 5.0[b]	113
tax-6(gf);ocr-2(yz5)	na	4.7[c]	35
tax-6(gf)	na	80.2 ± 5.2[d]	104
tax-6(gf);dyf-1(yz66)	na	222.6 ± 6.8[a]	118
Signaling mutants			
gpa-10;ocr-2(yz5)	na	5.6 ± 1.1[c]	23
gpa-10	na	108.4 ± 7.5[d]	38
gpa-10;bbs-7	na	314.0 ± 23.6[a]	38
gpa-13;ocr-2(yz5)	na	5.2 ± 0.2[c]	23
gpa-13;bbs-7;ocr-2(yz5)	na	97.5 ± 5.7[b]	39
goa-1;ocr-2(yz5)	na	6.3 ± 1.1[c]	23
goa-1	na	190.0 ± 10.3[a]	74
goa-1;che-2(e1033)	na	187.1 ± 9.2[d]	115
goa-1;che-2;ocr-2(yz5)	na	103.0 ± 6.2[b]	161
egl-30(lf);ocr-2(yz5)	na	5.1 ± 0.7[c]	29
egl-30(lf)	na	79.6 ± 5.4[d]	35
egl-30(gf)	na	70.7 ± 9.4[d]	31
eg-30(gf)	na	73.8 ± 13.7[d]	57
itr-1	na	86.0 ± 3.1[a]	201
unc-2;ocr-2(ak47)	na	5.5 ± 0.4[c]	23
unc-2	na	82.1 ± 2.5[a]	319

The data represent the fluorescence of the same *tph-1::gfp* transgene in different genetic backgrounds. L3–L4 larvae were analyzed. Each strain was analyzed in at least three independent experiments, with WT and mutants observed in parallel every time. The average pixel intensity in WT is defined as 100, and the average pixel intensity in other strains is normalized to WT assayed on the same day. *N*, Total number of animals per strain examined. DiI staining: +, dye-filling positive; −, dye-filling defective; na, not assayed.

[a]Significantly different from WT.

[b]Significantly different from *ocr-2*.

[c]Not significantly different from *ocr-2*.

[d]Not significantly different from WT.

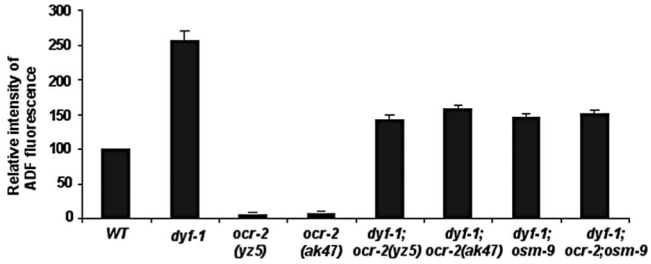

Figure 3. *tph-1::gfp* in the ADF neurons is upregulated in *dyf-1* mutants. Average fluorescence in the ADF neurons, normalized to that in WT, is shown for the mutants. L3 and L4 larvae were analyzed. Each bar represents the summary of three independent experiments ± SEM, with 10–15 animals per strain per experiment. There is a significant difference in the values between WT and *dyf-1* mutants ($p < 0.01$, Student's *t* test). However, there is no significant difference in the values among the double mutants ($p > 0.2$, Student's *t* test).

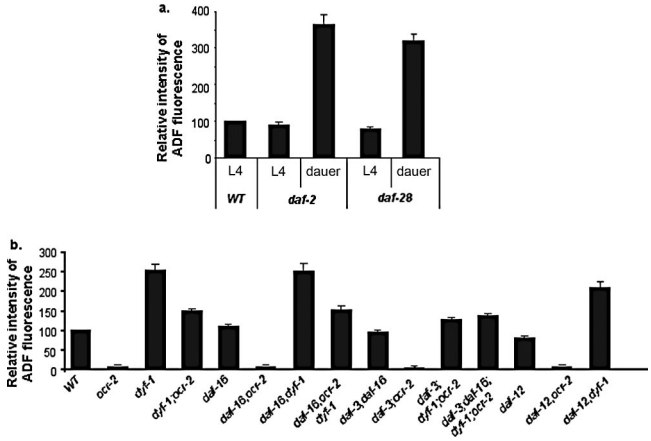

Figure 4. Quantification of *tph-1::gfp* expression in dauer-constitutive and dauer-defective mutants. Average fluorescence in the ADF neurons, normalized to that in WT grown under the same conditions and assayed in parallel, is shown for the mutants. ***a***, Dauer formation caused *tph-1::gfp* upregulation in mutants of *daf-2*/IGF-1 receptor and *daf-28*/IGF, compared with non-dauer *daf-2* and *daf-28* L4 larvae ($p < 0.01$, Student's *t* test). At 15°C and compared with age-matched WT, *tph-1::gfp* expression was not significantly changed in *daf-2* L4 ($p > 0.1$), but it was slightly reduced in *daf-28* L4 ($p = 0.03$, Student's *t* test). ***b***, Mutations in dauer-inducing transcription factors *daf-16*/FoxO, *daf-3*/SMAD, and *daf-12*/nuclear hormone receptor did not produce a significant effect on *tph-1::gfp* expression either on their own or in *ocr-2* and *dyf-1* mutant backgrounds ($p > 0.14$). However, the GFP intensity in *daf-3;dyf-1;ocr-2* was slightly lower than that in *dyf-1;ocr-2* ($p = 0.04$, Student's *t* test).

and DAF-12/nuclear hormone receptor (Hu, 2007). Like dauers, Dyf mutants accumulate DAF-16 in nuclei (Lin et al., 2001), indicating that DAF-16 is activated in Dyf mutants. We therefore investigated whether upregulation of *tph-1* is an outcome of activation of DAF-16.

We first tested whether activation of DAF-16 is sufficient to upregulate *tph-1* expression. DAF-16 nuclear accumulation is inhibited by signaling from the insulin growth factor-1 receptor DAF-2 (Lin et al., 1997; Ogg et al., 1997). Although *daf-2* reduction-of-function mutants constitutively accumulate DAF-16 in the nuclei, these *daf-2* mutants form dauers when grown at 26°C but not at 15°C (Hu, 2007), providing us a window to discern the effects of DAF-16 per se on *tph-1* expression. We crossed the same *tph-1::gfp* transgene into *daf-2(e1370)* mutants. At 15°C there was no significant difference between non-dauer *daf-2* mutants and age-matched WT animals in *tph-1::gfp* expression (Fig. 4*a*) or anti-5-HT immunoreactivity (data not shown), in contrast to a previous report (Estevez et al., 2006). Importantly, *daf-2* dauers showed increased *tph-1::gfp* expression in the

ADF neurons compared with that seen in WT dauers (Fig. 4*a*). The *daf-28* gene encodes an insulin-like peptide, and *daf-28(sa191)* mutants also form dauer mainly at 26°C (Li et al., 2003). *tph-1::gfp* expression in the ADF neurons was upregulated in *daf-28* dauers (Fig. 4*a*).

We next asked whether DAF-16 is required for *tph-1* upregulation in *dyf-1* mutants. We generated double mutants of *dyf-1* and *daf-16(mgDf50)* deletion, and found that lacking DAF-16 cannot prevent *tph-1::gfp* upregulation in *dyf-1* mutants (Fig. 4*b*). We tested further the effect of *daf-3* and *daf-12* on *tph-1* expression. A mutation in *daf-3* or in *daf-12* or a double mutation of *daf-3* and *daf-16* could not block upregulation of *tph-1::gfp* expression in *dyf-1* background (Fig. 4*b*). Furthermore, *daf-16*, *daf-16;daf-3*, and *daf-12* mutations did not downregulate *tph-1::gfp* expression on their own (Fig. 4*b*). Thus, activation of DAF-16, DAF-3, and DAF-12 cannot account for *tph-1* upregulation in *daf-2* and *daf-28* dauers or in IFT mutants.

Defective sensory functions per se are not sufficient to upregulate *tph-1* expression

IFT is essential for assembly and maintenance of the cilia of amphid chemosensory neurons, and IFT mutant worms are chemosensory defective (Perkins et al., 1986; Bargmann and Horvitz, 1991). To distinguish the role of the cilium morphology from sensory function of the neurons, we examined *tph-1::gfp* expression in mutants of sensory signaling components. The *tax-2/tax-4* cyclic nucleotide-gated channel is expressed in many amphid chemosensory neurons and is required for thermosensation, chemosensation, and gustatory sensation (Coburn and Bargmann, 1996; Komatsu et al., 1996). Mutants of calcineurin TAX-6 are broadly defective in sensation and adaptation to many environmental signals (Kuhara et al., 2002). However, unlike *dyf-1* and *dyf-12* mutations, mutants of *tax-2* and *tax-6* are not dye-filling defective, nor did they exhibit a significant effect on *tph-1::gfp* expression either on their own or in *ocr-2* mutant background (Table 1).

G-proteins regulate sensory signaling in the amphid neurons (Bastiani and Mendel, 2006). GOA-1 and Gq/EGL-30 have been shown to regulate *tph-1* expression in the HSN neurons (Tanis et al., 2008). Consistent with this report, we observed that *tph-1::gfp* expression in the ADF neurons was increased in *goa-1* mutants and reduced in *egl-30* mutants (Table 1). However, *goa-1* and *egl-30* mutations could not suppress *tph-1::gfp* downregulation in *ocr-2* mutants, nor could they block the upregulation in IFT mutants (Table 1). Furthermore, none of the mutations in four other Gα proteins expressed in ADF had an appreciable effect on *tph-1::gfp* expression on their own or in *ocr-2* and IFT mutant backgrounds (Table 1) (S. Zhang et al., 2004). The opposite effects of *goa-1* and *egl-30* mutations support the idea of an antagonistic action on *tph-1* expression in the ADF neurons. However, dysfunction of *goa-1* or *egl-30* cannot fully account for *tph-1::gfp* upregulation observed in dauers and IFT mutants. In addition, mutations in *unc-2*, which encodes the α subunit of a voltage-gated calcium channel and regulates synaptic properties of the amphid neurons (Troemel et al., 1999), and mutation in a calcium signaling component *itr-1* did not produce a significant effect on *tph-1::gfp* expression (Table 1) or 5-HT immunoreactivity (data not shown). Collectively, these results suggest that sensory deficits are unlikely to be a trigger of *tph-1::gfp* upregulation in IFT mutants.

Hedgehog-like signaling components coordinate changes in cilium morphology and *tph-1* expression

Studies with *Drosophila* and mammalian systems have revealed an intimate interplay between IFT and Hh signaling (Huangfu et al., 2003; Corbit et al., 2005; Tran et al., 2008). While no conventional *C. elegans* Hh homolog can be recognized, the *C. elegans* genome encodes 10 Hh-like proteins (Hao et al., 2006). Importantly, *daf-6*, a homolog of Hh receptor Patched, and *che-14*, a homolog of Hh-releasing factor Dispatched, function in the sheath glia and the socket cells and influence cilium structure of the amphid sensory neurons (Perkins et al., 1986; Michaux et al., 2000; Perens and Shaham, 2005). *daf-6* and *che-14* mutants accumulate densely stained secretory vesicles within the sheath glia, exhibit obstructed amphid channel and misplacement and bending of the sensory cilia, and are dye-filling defective. Conversely, IFT mutants alter DAF-6 subcellular localization and amphid channel morphology (Perkins et al., 1986; Perens and Shaham, 2005). We therefore analyzed *tph-1::gfp* in *daf-6* and *che-14* mutants. Both *daf-6* and *che-14* mutants exhibited *tph-1::gfp* upregulation on their own as well as in *ocr-2* mutant background (Table 1). Thus, IFT deficits in the sensory cilia or inactivation of an Hh-like activity in the amphid channel can both alter the amphid structure and trigger the signaling pathway to upregulate *tph-1* expression in the ADF neurons.

Dauers alter the expression of Patched DAF-6

EM showed that the amphid morphology of *daf-6* and *che-14* mutants resembles that seen in WT dauers (Albert and Riddle, 1983). To test the possibility that DAF-6 activity underscores amphid structural plasticity, we examined the expression of GFP-tagged DAF-6 protein (DAF-6::GFP) in dauers. DAF-6::GFP was expressed in the sheath and socket cells, as well as in the excretory canal at all stages of animals (Fig. 5*a*) (Perens and Shaham, 2005). In dauers, DAF-6::GFP expression in these cells was dramatically reduced/eliminated, although a pair of small puncta at the tip of the sheath cells remained in some animals (Fig. 5), and most of the animals failed dye filling. At the same time, DAF-6::GFP co-localized with a dauer-specific cuticular structure called dauer alae (Fig. 5*a*). DAF-6::GFP expression in the sheath and socket cells was fully restored within 24 h when dauers were allowed to recover under optimal growth conditions (Fig. 5*b*), coincident with recovery of dye filling. These results indicate that dauers remodel the expression pattern of DAF-6, and reduction in DAF-6 expression in the amphids correlates with changes in the cilium architecture and upregulation of *tph-1::gfp* expression.

cGMP functions in the pathway upregulating *tph-1* expression

cGMP is a second messenger of cilium-generated signaling in mammalian auditory, visual, and olfactory systems (Bradley et al., 2005; Salathe, 2007). It has been reported that the dauer-defective phenotype of *daf-6* and *che-14* can be suppressed by mutations in the guanylyl cyclase *daf-11* (Birnby et al., 2000), indicating that inactivation of DAF-6 and CHE-14 inappropriately turns on cGMP signaling. The *C. elegans* genome encodes >30 guanylyl cyclases, although *daf-11* is not expressed in the ADF neurons (Yu et al., 1997; Birnby et al., 2000). As the first step toward understanding the molecular mechanism that couples the Hh-related signaling, cilium structure, and regulated-5-HT production, we tested whether increased cGMP can trigger *tph-1::gfp* upregulation in the ADF neurons. We examined *tph-1::gfp* expression in *ocr-2* mutants grown on culture plates supplied with the membrane-permeable cGMP analog 8-bromo-cGMP. We

observed a cGMP dosage-dependent increase in *tph-1::gfp* expression (Table 2). At 2.5 mM, *tph-1::gfp* in the ADF neurons was distinctly observed in 65% of *ocr-2(yz5)* and 80% of *ocr-2(ak47)*, whereas the expression was not visible in 77–98% of age-matched, drug-free controls (Table 2). While this study is not sufficient to establish a cGMP function in the ADF neurons, the result suggests that cGMP is a component in the pathway leading to *tph-1* upregulation.

IFT mutations decouple aversive experience and *tph-1* expression

To determine whether changes in cilium morphology are relevant to stress-induced *tph-1* upregulation, we observed *tph-1::gfp* expression in *dyf-1* dauers. High growth temperature can induce IFT mutants to form dauers (Ailion and Thomas, 2000). However, *tph-1::gfp* expression in the ADF neurons was not further increased in *dyf-1* or *dyf-1;ocr-2* dauers (Fig. 6*a*).

We further investigated whether the parallel changes in *tph-1* expression and amphid structure can be induced by other aversive experiences. Heat shock is another extreme stress for worms (Lithgow et al., 1995). WT worms die after they are incubated at 37.5°C for 3 h. But some of worms survive when they are incubated at 37.5°C for 1.5 h. We incubated worms at 37.5°C for 1.5 h, then transferred them back to the optimal growth temperature of 20°C, and *tph-1::gfp* expression in survivors was examined 7 h later. *tph-1::gfp* expression in the ADF neurons was significantly upregulated in survived WT and *ocr-2* mutants (Fig. 6*b*).

We next examined amphid structure in these heat-shock survivors, using dye-filling assays. Approximately 10% of survived WT animals completely failed in dye filling with DiI, and most of the animals showed reduced staining. We further analyzed *tph-1::gfp* expression in IFT mutants after the heat shock treatment. Heat shock did not induce *tph-1::gfp* upregulation in *dyf-1* mutants either on their own or in *ocr-2* mutant background (Fig. 6*b*). These results demonstrate that dendritic cilium morphology in the amphids can be modified by several aversive conditions, that cilium structural modification correlates with *tph-1* upregulation in the ADF chemosensory neurons, and that IFT mutants decouple *tph-1* expression and the aversive conditions.

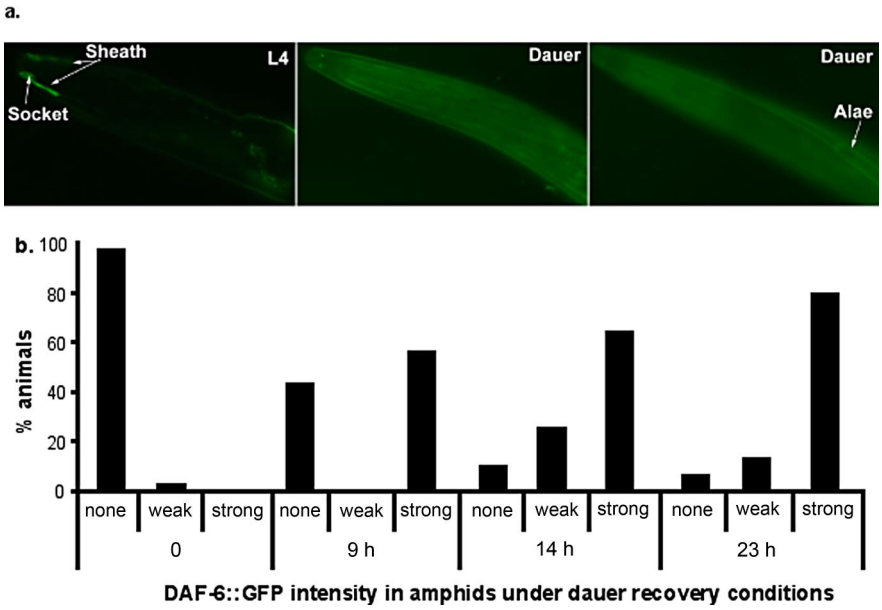

Figure 5. Dauers remodel the expression of DAF-6 Patched. ***a***, Photomicrographs of GFP-tagged DAF-6 protein (DAF-6::GFP) in WT animals. DAF-6::GFP was observed in the sheath and socket cells in L4 larvae. In dauers, DAF-6::GFP expression in the sheath and socket cells was dramatically reduced but colocalized with the dauer alae. All animals shown have anterior toward the left. ***b***, Expression of DAF-6::GFP in the sheath and socket cells was progressively restored when WT animals recovered from the dauer stage. The definitions of GFP levels are as follows: strong, WT L4 levels as shown in the left panel of ***a***; weak, fluorescence in characteristic sheath and socket cells can be identified; none, the characteristic structure of these cells cannot be recognized. The numbers shown are from a single experiment, with 30–40 animals assayed for each time point. Experiments repeated on independent days show similar relative differences.

Table 2. Effects of 8-bromo-cGMP on *tph-1::gfp* expression in ADF

		tph-1::gfp expression in ADF	
Strains	8-Bromo-cGMP (mM)	Very weak/invisible (*N*)	Medium/strong (*N*)
WT		0	17
	1.25	0	40
	2.50	0	26
ocr-2(yz5)		50	1
	1.25	70	10
	2.50	34	62
ocr-2(ak47)		27	8
	1.25	15	14
	2.50	10	39

Eggs from a strain were laid on NGM plates containing 8-bromo-cGMP at indicated concentrations and incubated at 20° C, and *tph-1::gfp* in hatched animals was analyzed 48 h later. The definitions of GFP levels are as follows: strong, WT levels as shown in Figure 2*c*; medium, the ADF cell body can be clearly recognized; very weak/invisible, ADF cell body is not discernible. *N*, Number of animals in each category examined. The results are based on one trial of *ak47* and two independent trials of *yz5*.

Discussion

Fluctuations of neuronal 5-HT levels have been shown to produce a profound impact on learning and adaptation to aversive environment in both vertebrates and invertebrates (Kandel, 2001). In this paper, we provide genetic evidence that 5-HT biosynthesis in a pair of ADF chemosensory neurons in *C. elegans* is coupled to the environment through dynamic changes in cilium architecture of the neurons, and this cilium structural plasticity is regulated at least in part by DAF-6, a homolog of Hh receptor Patched. Our findings are corroborated by EM analyses, which have shown similar amphid structural modifications in IFT and Hh-like signaling mutants and in WT animals under stress such as dauer-inducing conditions (Albert and Riddle, 1983; Perkins et al., 1986), and the recent work demonstrating the cilium structural plasticity regulated by neural activity (Mukhopadhyay et al., 2008). Interplay between IFT and Hh signaling has been shown to regulate pattern formation and in particular the development of 5-HT phenotypes in mammalian brains. Our work demonstrates that IFT machinery and Hh-like signaling coordinate sensory architecture and gene expression of 5-HT neurons in living animals according to the environment. However, there appears to be a distinction between the signaling of IFT and Hh in mouse development and that in *C. elegans* amphids. In mouse studies, both IFT machinery and Patched appeared to function cell autonomously (Huangfu et al., 2003; Corbit et al., 2005; Tran et al., 2008). The results from our work indicate that DAF-6 acts in the amphid channel surrounding the cilia, whereas IFT acts cell autonomously to regulate *tph-1* expression, thereby regulating 5-HT biosynthesis in the sensory neurons.

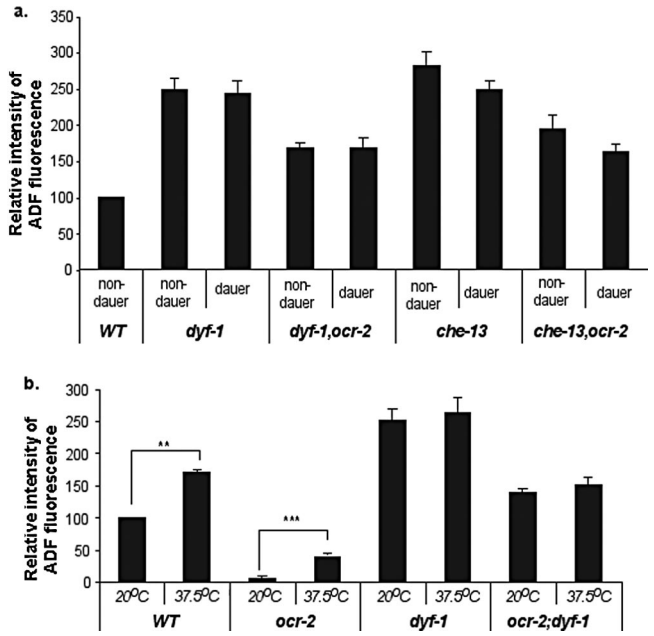

Figure 6. The effects of dauer formation and heat shock stress on *tph-1::gfp* expression in IFT mutant backgrounds. ***a***, Average GFP fluorescence in the ADF neurons, normalized to that in WT L3–L4 grown at 20°C, is shown for mutants. For a given Dyf strain, there is no significant difference between the values in dauers and non-dauers ($p > 0.2$, Student's *t* test). ***b***, Average GFP fluorescence in the ADF neurons, normalized to that in WT controls at 20°C, is shown for WT heat-shock survivors and the mutants. Heat shock treatment induced *tph-1::gfp* upregulation in WT (**$p < 0.01$) and *ocr-2* mutants (***$p < 1.3 \times 10^{-6}$), but not in *dyf-1* and *dyf-1;ocr-2* double mutants ($p > 0.35$), all based on Student's *t* test. Each bar represents the summary of three independent experiments ± SEM, with 10–15 animals per strain per experiment.

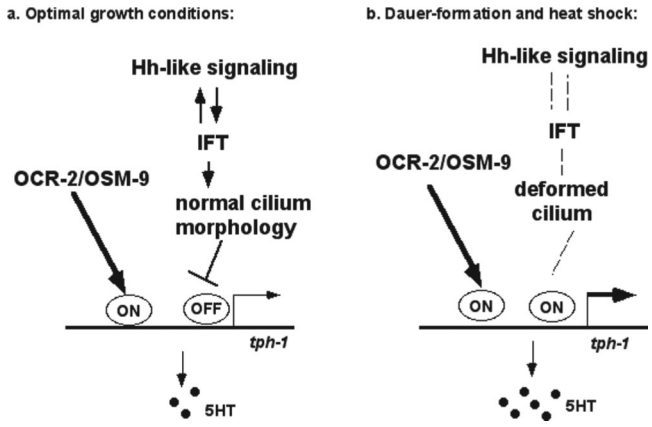

Figure 7. A model for a two-layer transcriptional activation of *tph-1* expression in the ADF neurons. ***a***, Under optimal growth conditions, TRPV signaling is required to turn on *tph-1* expression, whereas IFT/Hh-like signaling represses *tph-1* expression via an independent mechanism. ***b***, In dauers and heat-shock survivors, IFT/Hh-like signaling is perturbed, which alters the cilium architecture of the ADF neurons, resulting in derepression of *tph-1* expression. As the TRPV channel continues at work, *tph-1* expression is upregulated to catalyze more 5-HT biosynthesis.

A variety of stress alters 5-HT production

As in mammals, 5-HT is continuously produced in *C. elegans*. Analysis of *tph-1::gfp* expression in specific cells has led to the discovery of many genes and cues that modulate *tph-1* expression, and, therefore, 5-HT production in animals undertaking complex behavior. Several results from this work suggest that IFT and Hh-like signaling and OCR-2/OSM-9 TRPV channel regulate two layers of activation of *tph-1* expression (Fig. 7). First, *tph-1::gfp* expression in ADF was downregulated in *ocr-2* and *osm-9* mutants. Although *tph-1::gfp* expression in *ocr-2* and *osm-9* mutant dauers was increased relative to their non-dauer siblings, the expression levels were significantly lower than that seen in WT dauers. This suggests that the signaling from the TRPV channel activates *tph-1* expression under both optimal growth conditions and dauer-inducing conditions. Second, *tph-1::gfp* expression in ADF was further upregulated in dauers and mutants of IFT/Hh-like signaling. This suggests that IFT and Hh-like signaling normally represses *tph-1* expression. Because WT dauers and IFT mutants can upregulate *tph-1* expression in *ocr-2;osm-9* double-null mutant background, dauers and IFT mutants enhance *tph-1* expression via a mechanism genetically separable from the TRPV channel. Third, expression of *dyf-1* in the ADF neurons was required to revert *tph-1::gfp* upregulation in *dyf-1* mutants. This suggests that IFT in ADF cilium and/or cilium structure of the ADF neurons respond to the Hh-like signaling. Because dauer formation and heat shock could not further enhance *tph-1* expression in *dyf-1* mutants, this supports the model in which these aversive conditions upregulate *tph-1* expression by derepressing the mechanism regulated by IFT, and that IFT mutants constitutively derepress the mechanism. This idea is consistent with the findings of increased stress response genes in IFT mutants (Lin et al., 2001). Previously, it has been shown that *tph-1* expression in the ADF neurons is increased in TGF-β/*daf-7* mutants, but this *tph-1* enhancement requires DAF-3 (Chang et al., 2006), whereas *tph-1* upregulation in WT dauers and IFT/Hh signaling mutants is independent of DAF-3 or other known dauer-inducing transcription factors. *tph-1* expression in ADF is also enhanced in WT animals exposed to pathogenic bacteria (Y. Zhang et al., 2005). On the other hand, all these circumstances do not have a significant effect on *tph-1* expression in any other 5-HT neurons of the animal. These observations demonstrate a remarkable cell specificity in regulating 5-HT production, making it more striking that a variety of stress acts via multiple genetic pathways converging on the promoter of *tph-1* within the sole 5-HT chemosensory neurons in the animal.

The increased 5-HT production induced by dauer formation and heat shock in *C. elegans* may be relevant to the response of mammalian brains to uncontrollable stress. Uncontrollable stress describes acute stresses that lead to a constellation of behavioral and physiological modifications (Maier and Watkins, 2005). In rats, the same stressors may upregulate 5-HT signaling under uncontrollable conditions but not under controllable conditions (Grahn et al., 1999). The dauer formation is a result of a series of structural and functional modifications of both the neuronal and non-neuronal systems induced by compound aversive environmental conditions. In this paper, we show that *tph-1* mutants are delayed in dauer recovery compared with WT. This result is consistent with a published work (Daniels et al., 2000) demonstrating that applying exogenous 5-HT can promote dauer recovery. It may be sensible that an increase in 5-HT signaling under uncontrollable stress is a mechanism selected in evolution for animals to learn and cope with the harsh reality and to recover when possible. This mechanism could underscore a role of antidepressants in alleviating aversive consequences of uncontrollable stress in rodents and the positive effects of the drugs on depression in humans.

IFT and Hh signaling regulate 5-HT production

Our genetic analyses revealed that IFT in the dendritic cilium of ADF is a mediator to repress *tph-1* upregulation, but Hh-related factors in the amphid channel are critical in the process. Both

daf-6/Patched and *che-14/Dispatched* are expressed in the sheath and socket cells that form a channel wrapping around the cilia of ADF and other chemosensory neurons in the amphids (Michaux et al., 2000; Perens and Shaham, 2005). These results suggest that the amphid channel provides a cue to ADF and regulated-*tph-1* expression.

We can envision at least two mechanisms by which DAF-6 and CHE-14 influence *tph-1* expression in the ADF neurons. First, DAF-6 and CHE-14 control the morphology of the amphid channel, which shapes the architecture of ADF cilia, analogous to the Müller cells and pigment epithelium surrounding the cilia of photoreceptors and the phalangeal cells and tectorial membrane surrounding hair cells in the cochlear duct. It is plausible that, like photoreceptors and hair cells, deformation of ADF cilium triggers neural activity, leading to *tph-1* upregulation. This idea is supported by the fact that *tph-1* upregulation in WT dauers, heat-shock survivors, and the mutants all are accompanied by a deformed amphid. Interestingly, we found that an analog of cGMP, the major second messenger of the photoreceptors and hair cells, can induce *tph-1* expression in ADF in *ocr-2* mutant backgrounds under optimal growth conditions. One attractive possibility is that alterations in ADF cilia trigger a cGMP signaling, leading to upregulation of *tph-1* expression.

Second, DAF-6 and CHE-14 may regulate the secretion of Hh-like peptides with signaling activity. The *C. elegans* genome encodes 10 Hh-like peptides that exhibit similarities to the Hh protein at the C-terminal autoprocessing domain but have novel N-terminal sequences (Hao et al., 2006). The Hh autoprocessing domain catalyzes the intramolecular cleavage and transfers cholesterol to the cleaved N-terminal signaling domain. Thus, it remains possible that DAF-6 and CHE-14 secrete a sterol-modified peptide that interacts with ADF cilium and regulate *tph-1* expression. It is intriguing that dauers also induce *tph-1* expression ectopically in the ventral cord motor neurons, because in mouse brain motor neurons and 5-HT neurons are generated from a common pool of progenitors and dysregulation of Hh downstream transcriptional cascade causes the motor neurons to express 5-HT phenotype (Pattyn et al., 2003). Although the exact mechanism by which Hh-like signaling regulates *tph-1* expression is not known, our study established a genetic correlation between Hh-like signaling molecules, IFT in the sensory cilia of 5-HT neurons, and regulated 5-HT production. Thus, despite the divergence on signaling molecules involved, the strategy used to determine the identity of 5-HT neurons in mammals may be conserved in *C. elegans* to regulate the morphological plasticity of 5-HT neurons according to the environment.

References

Ailion M, Thomas JH (2000) Dauer formation induced by high temperatures in *Caenorhabditis elegans.* Genetics 156:1047–1067.

Albert PS, Riddle DL (1983) Developmental alterations in sensory neuroanatomy of the *Caenorhabditis elegans* dauer larva. J Comp Neurol 219:461–481.

Apfeld J, Kenyon C (1999) Regulation of lifespan by sensory perception in *Caenorhabditis elegans*. Nature 402:804–809.

Azmitia EC (1999) Serotonin neurons, neuroplasticity, and homeostasis of neural tissue. Neuropsychopharmacology 21:33S–45S.

Bargmann CI, Horvitz HR (1991) Chemosensory neurons with overlapping functions direct chemotaxis to multiple chemicals in *C. elegans.* Neuron 7:729–742.

Bastiani C, Mendel J (2006) Heterotrimeric G proteins in *C. elegans.* In: WormBook (The *C. elegans* Research Community, ed.), doi/10.1895/wormbook.1.75.1, http://www.wormbook.org.

Birnby DA, Link EM, Vowels JJ, Tian H, Colacurcio PL, Thomas JH (2000) A transmembrane guanylyl cyclase (DAF-11) and Hsp90 (DAF-21) regulate a common set of chemosensory behaviors in *Caenorhabditis elegans.* Genetics 155:85–104.

Blacque OE, Perens EA, Boroevich KA, Inglis PN, Li C, Warner A, Khattra J, Holt RA, Ou G, Mah AK, McKay SJ, Huang P, Swoboda P, Jones SJ, Marra MA, Baillie DL, Moerman DG, Shaham S, Leroux MR (2005) Functional genomics of the cilium, a sensory organelle. Curr Biol 15:935–941.

Bradley J, Reisert J, Frings S (2005) Regulation of cyclic nucleotide-gated channels. Curr Opin Neurobiol 15:343–349.

Brenner S (1974) The genetics of *Caenorhabditis elegans.* Genetics 77:71–94.

Briscoe J, Sussel L, Serup P, Hartigan-O'Connor D, Jessell TM, Rubenstein JL, Ericson J (1999) Homeobox gene Nkx2.2 and specification of neuronal identity by graded Sonic hedgehog signalling. Nature 398:622–627.

Cassada RC, Russell RL (1975) The dauerlarva, a post-embryonic developmental variant of the nematode *Caenorhabditis elegans.* Dev Biol 46:326–342.

Chang AJ, Chronis N, Karow DS, Marletta MA, Bargmann CI (2006) A distributed chemosensory circuit for oxygen preference in *C. elegans.* PLoS Biol 4:e274.

Chaouloff F (2000) Serotonin, stress and corticoids. J Psychopharmacol 14:139–151.

Coburn CM, Bargmann CI (1996) A putative cyclic nucleotide-gated channel is required for sensory development and function in *C. elegans.* Neuron 17:695–706.

Corbit KC, Aanstad P, Singla V, Norman AR, Stainier DY, Reiter JF (2005) Vertebrate Smoothened functions at the primary cilium. Nature 437:1018–1021.

Daniels SA, Ailion M, Thomas JH, Sengupta P (2000) egl-4 acts through a transforming growth factor-beta/SMAD pathway in *Caenorhabditis elegans* to regulate multiple neuronal circuits in response to sensory cues. Genetics 156:123–141.

Estevez AO, Cowie RH, Gardner KL, Estevez M (2006) Both insulin and calcium channel signaling are required for developmental regulation of serotonin synthesis in the chemosensory ADF neurons of *Caenorhabditis elegans.* Dev Biol 298:32–44.

Golden JW, Riddle DL (1984) The *Caenorhabditis elegans* dauer larva: developmental effects of pheromone, food, and temperature. Dev Biol 102:368–378.

Grahn RE, Maswood S, McQueen MB, Watkins LR, Maier SF (1999) Opioid-dependent effects of inescapable shock on escape behavior and conditioned fear responding are mediated by the dorsal raphe nucleus. Behav Brain Res 99:153–167.

Hao L, Mukherjee K, Liegeois S, Baillie D, Labouesse M, Bürglin TR (2006) The hedgehog-related gene *qua-1* is required for molting in *Caenorhabditis elegans.* Dev Dyn 235:1469–1481.

Huangfu D, Liu A, Rakeman AS, Murcia NS, Niswander L, Anderson KV (2003) Hedgehog signalling in the mouse requires intraflagellar transport proteins. Nature 426:83–87.

Hu PJ (2007) Dauer. In: WormBook (The *C. elegans* Research Community, ed.), doi/10.1895/wormbook.1.144.1, http://www.wormbook.org.

Ingham PW, McMahon AP (2001) Hedgehog signaling in animal development: paradigms and principles. Genes Dev 15:3059–3087.

Inglis PN, Ou G, Leroux MR, Scholey JM (2007) The sensory cilia of *Caenorhabditis elegans.* In: WormBook (The *C. elegans* Research Community, ed.), doi/10.1895/wormbook.1.126.1, http://www.wormbook.org.

Jansen G, Hazendonk E, Thijssen KL, Plasterk RH (1997) Reverse genetics by chemical mutagenesis in *Caenorhabditis elegans.* Nat Genet 17:119–121.

Kandel ER (2001) The molecular biology of memory storage: a dialogue between genes and synapses. Science 294:1030–1038.

Komatsu H, Mori I, Rhee JS, Akaike N, Ohshima Y (1996) Mutations in a cyclic nucleotide-gated channel lead to abnormal thermosensation and chemosensation in *C. elegans.* Neuron 17:707–718.

Kuhara A, Inada H, Katsura I, Mori I (2002) Negative regulation and gain control of sensory neurons by the *C. elegans* calcineurin TAX-6. Neuron 33:751–763.

Lee EH, Lin HH, Yin HM (1987) Differential influences of different stressors upon midbrain raphe neurons in rats. Neurosci Lett 80:115–119.

Leonardo ED, Hen R (2006) Genetics of affective and anxiety disorders. Annu Rev Psychol 57:117–137.

Li W, Kennedy SG, Ruvkun G (2003) *daf-28* encodes a *C. elegans* insulin superfamily member that is regulated by environmental cues and acts in the DAF-2 signaling pathway. Genes Dev 17:844–858.

Lin K, Dorman JB, Rodan A, Kenyon C (1997) *daf-16*: An HNF-3/forkhead family member that can function to double the life-span of *Caenorhabditis elegans.* Science 278:1319–1322.

Lin K, Hsin H, Libina N, Kenyon C (2001) Regulation of the *Caenorhabditis elegans* longevity protein DAF-16 by insulin/IGF-1 and germline signaling. Nat Genet 28:139–145.

Lithgow GJ, White TM, Melov S, Johnson TE (1995) Thermotolerance and extended life-span conferred by single-gene mutations and induced by thermal stress. Proc Natl Acad Sci U S A 92:7540–7544.

Maier SF, Watkins LR (2005) Stressor controllability and learned helplessness: the roles of the dorsal raphe nucleus, serotonin, and corticotropin-releasing factor. Neurosci Biobehav Rev 29:829–841.

Michaux G, Gansmuller A, Hindelang C, Labouesse M (2000) CHE-14, a protein with a sterol-sensing domain, is required for apical sorting in *C. elegans* ectodermal epithelial cells. Curr Biol 10:1098–1107.

Mukhopadhyay S, Lu Y, Shaham S, Sengupta P (2008) Sensory signaling-dependent remodeling of olfactory cilia architecture in *C. elegans.* Dev Cell 14:762–774.

Ogg S, Paradis S, Gottlieb S, Patterson GI, Lee L, Tissenbaum HA, Ruvkun G (1997) The Fork head transcription factor DAF-16 transduces insulin-like metabolic and longevity signals in *C. elegans.* Nature 389:994–999.

Ottaviani E, Franceschi C (1996) The neuroimmunology of stress from invertebrates to man. Prog Neurobiol 48:421–440.

Ou G, Blacque OE, Snow JJ, Leroux MR, Scholey JM (2005) Functional coordination of intraflagellar transport motors. Nature 436:583–587.

Pattyn A, Vallstedt A, Dias JM, Samad OA, Krumlauf R, Rijli FM, Brunet JF, Ericson J (2003) Coordinated temporal and spatial control of motor neuron and serotonergic neuron generation from a common pool of CNS progenitors. Genes Dev 17:729–737.

Peckol EL, Troemel ER, Bargmann CI (2001) Sensory experience and sensory activity regulate chemosensory receptor gene expression in *Caenorhabditis elegans.* Proc Natl Acad Sci U S A 98:11032–11038.

Perens EA, Shaham S (2005) *C. elegans* daf-6 encodes a patched-related protein required for lumen formation. Dev Cell 8:893–906.

Perkins LA, Hedgecock EM, Thomson JN, Culotti JG (1986) Mutant sensory cilia in the nematode *Caenorhabditis elegans.* Dev Biol 117:456–487.

Rosenbaum JL, Witman GB (2002) Intraflagellar transport. Nat Rev Mol Cell Biol 3:813–825.

Rubenstein JL (1998) Development of serotonergic neurons and their projections. Biol Psychiatry 44:145–150.

Sagasti A, Hobert O, Troemel ER, Ruvkun G, Bargmann CI (1999) Alternative olfactory neuron fates are specified by the LIM homeobox gene *lim-4.* Genes Dev 13:1794–1806.

Salathe M (2007) Regulation of mammalian ciliary beating. Annu Rev Physiol 69:401–422.

Scholey JM (2003) Intraflagellar transport. Annu Rev Cell Dev Biol 19:423–443.

Scholey JM, Anderson KV (2006) Intraflagellar transport and cilium-based signaling. Cell 125:439–442.

Starich TA, Herman RK, Kari CK, Yeh WH, Schackwitz WS, Schuyler MW, Collet J, Thomas JH, Riddle DL (1995) Mutations affecting the chemosensory neurons of *Caenorhabditis elegans.* Genetics 139:171–188.

Sze JY, Victor M, Loer C, Shi Y, Ruvkun G (2000) Food and metabolic signalling defects in a *Caenorhabditis elegans* serotonin-synthesis mutant. Nature 403:560–564.

Tanis JE, Moresco JJ, Lindquist RA, Koelle MR (2008) Regulation of serotonin biosynthesis by the G proteins Galphao and Galphaq controls serotonin signaling in *Caenorhabditis elegans.* Genetics 178:157–169.

Tran PV, Haycraft CJ, Besschetnova TY, Turbe-Doan A, Stottmann RW, Herron BJ, Chesebro AL, Qiu H, Scherz PJ, Shah JV, Yoder BK, Beier DR (2008) THM1 negatively modulates mouse sonic hedgehog signal transduction and affects retrograde intraflagellar transport in cilia. Nat Genet 40:403–410.

Troemel ER, Sagasti A, Bargmann CI (1999) Lateral signaling mediated by axon contact and calcium entry regulates asymmetric odorant receptor expression in *C. elegans.* Cell 99:387–398.

Ward S, Thomson N, White JG, Brenner S (1975) Electron microscopical reconstruction of the anterior sensory anatomy of the nematode *Caenorhabditis elegans.* J Comp Neurol 160:313–337.

Yu S, Avery L, Baude E, Garbers DL (1997) Guanylyl cyclase expression in specific sensory neurons: a new family of chemosensory receptors. Proc Natl Acad Sci USA 94:3384–3387.

Zhang S, Sokolchik I, Blanco G, Sze JY (2004) *Caenorhabditis elegans* TRPV ion channel regulates 5HT biosynthesis in chemosensory neurons. Development 131:1629–1638.

Zhang Y, Lu H, Bargmann CI (2005) Pathogenic bacteria induce aversive olfactory learning in *Caenorhabditis elegans.* Nature 438:179–184.